NANOPHOTOPOLYMERIZATION TRIGGERED BY THE ENHANCED OPTICAL NEAR-FIELD OF METALLIC NANOPARTICLES

Claire Deeb, Libai Huang[1], Jérôme Plain, Alexandre Bouhelier[2], Olivier Soppera[3], Renaud Bachelot and Pascal Royer
Laboratoire de Nanotechnologie et d'Instrumentation Optique LNIO-ICD FRE CNRS 2848, Université de Technologie de Troyes, Troyes, France
[1] Radiation Laboratory, University of Notre Dame, Indiana, USA
[2] Institut Interdisciplinaire Carnot de Bourgogne CNRS-UMR 5209, Université de Bourgogne, Dijon, France
[3] Institut de Science des Matériaux de Mulhouse (IS2M-CNRS LCR 7228), Université de Haute-Alsace, Mulhouse, France
claire.deeb@utt.fr

ABSTRACT

A novel approach is reported for imaging and quantifying both the depth and the strength of the optical near-field, of a single colloidal metal nanoparticle, associated with localized surface plasmons. It will be emphasized that this technique relies on a nanoscale molecular molding of the confined electromagnetic field of metal colloids, irradiated at their resonance, by a photo-activated polymer, which enabled us to directly image the dipolar profile of the near-field distribution with an unprecedented resolution, better than 10 nm. Moreover, the approach used enabled one to quantify the near-field enhancement factor.

This approach has overcome all the difficulties faced by scanning probe methodologies to reproduce the form of the near-field of the localized surface plasmons and provides a new way to quantify its magnitude. Furthermore, this approach leads to the production of polymer/metal hybrid nano-systems of new optical properties.

Keywords: nanoantenna, nanoscale photopolymerization, localized surface plasmons, near field, hybrid nano-systems

INTRODUCTION

The optical properties of metal nanoparticles (MNP) have been the subject of extensive experimental and theoretical research for a long time (Zayat & Smolyaninov, 2003; Barnes *et al*., 2003; Schuller *et al*., 2010). The most important optical phenomenon encountered in these metallic structures is their electromagnetic surface plasmon resonance (SPR) due to collective oscillations of the conduction electrons. The localized surface plasmons (LSP) are responsible for molecular labeling (Bachelot *et al*., 2003), nanoscale optical field enhancement (Ibn El Ahrach *et al*., 2007), photoluminescence (Bouhelier *et al*.,

2005), solar energy harvesting (Atwater & Polman, 2010), photothermal tumor ablation (Haes *et al*., 2004), efficient light generation (Noginov *et al*., 2009), and diverse other applications. For all the applications assigned to the MNP, a precise control of their optical properties is necessary, which specially concerns the spectral LSP resonance position. A detailed understanding of the near-field response of engineered plasmonic nanostructures is therefore essential for controlling and optimizing a desired outcome along the line of the applications listed above. Determining a simple method for an accurate nanometer scale imaging of confined optical fields with quantitative measurements still constitutes an opened challenge.

In this paper a new technique is presented that enables one to fabricate polymer/metal hybrid nano-systems with new optical properties. This approach is based on controlled nanoscale photopolymerization triggered by local enhanced electromagnetic fields of metallic particles. Silver colloidal nanoparticles (CNP) were chosen in a way to achieve mutual spectral overlapping between their SPR, when embedded in liquid monomer, and photopolymer absorption. The glass slide was functionalized to create an amine-terminated self-assembled monolayer on which CNP were dispersed and strongly bounded to the glass surface.

In parallel, a photosensitive formulation is firstly developed and is subsequently characterized by an Argon-Krypton laser source coupled to an inverted optical microscope, in order to determine its threshold dose of photopolymerization. A drop of liquid photopolymerizable formulation was deposited on the substrate. Photopolymerization relies on production of free radicals and is characterized by a nonlinear threshold behavior allowing for high resolution patterning. After formulation deposition, the sample was illuminated in such a way that the incident energy was below the threshold so that polymerization occurs only around MNP where local near-fields are enhanced.

Three main points have to be mentioned here: first, this approach opens the door to nanophotochemistry of polymers. Second, it constitutes a new way of quantifying the field enhancement associated with localized surface plasmon resonance. Third, it allows for control of the optical properties of the MNP: the spatially inhomogeneous electromagnetic intensity distribution enhanced by the underlying surface plasmon leads to an anisotropic polymerization around the particles, introducing thus a degree of SPR tunability.

While further experiments are under way, the data presented in this paper concern mainly the development of a new experimental setup and the irradiation of CNP with different incident doses in order to quantify the near-field enhancement associated with LSP.

This paper is organized as follows: the section "Materials and Methods" firstly describes the new experimental setup that has been developed to establish different exposure configurations of the CNP. Then, the photopolymerization principle and reaction mechanism of the chemical system is fully detailed together with its composition. The procedure followed to functionalize the glass slides and to end up with a well distributed CNP configuration is also emphasized in this section. Exposure of CNP with different incident doses and the results obtained are discussed and detailed in the section "Results and Discussion". A conclusion will end this paper.

MATERIALS AND METHODS

Experimental setup

The newly experimental setup is represented in Figure 1. This setup has been developed after receiving the equipments (Ar:Kr laser source, inverted optical microscope, AFM, *etc*…) financed by the ANR, under grant Photohybrid (BLANC 07-2-188654).

The actinic light is delivered by a multi rays, ranging from 454 nm to 647 nm, Ar:Kr laser source that is first coupled in a single mode optical fiber. Coupling in the optical fiber guarantees a quite filtered, cleaned and presenting a Gaussian profile laser beam. The beam is then collimated by means of an objective with 0.12 as NA. The chosen incident wavelength should lie in the absorption spectrum of the dye of the chemical formulation. The beam is then reflected through a couple of mirrors, passes through a polarizer to adjust the polarization of the incident beam, and is finally coupled to an optical inverted microscope Olympus Ix71. Prior to the optical microscope, a 50/50 beam splitter is utilized to reflect part of the beam to an optical power meter so that the power of the excitation beam is constantly monitored for any fluctuation. The diameter of the laser spot, at the level of the sample stage, after a 0.6 NA objective can be adjusted between 3 μm and 8 μm by placing a pinhole through the path of the laser beam. Obviously, the diameter of the spot can be reduced more by increasing the NA of the microscope objective; with 1.45 NA, a spot of 250 nm as diameter was reached.
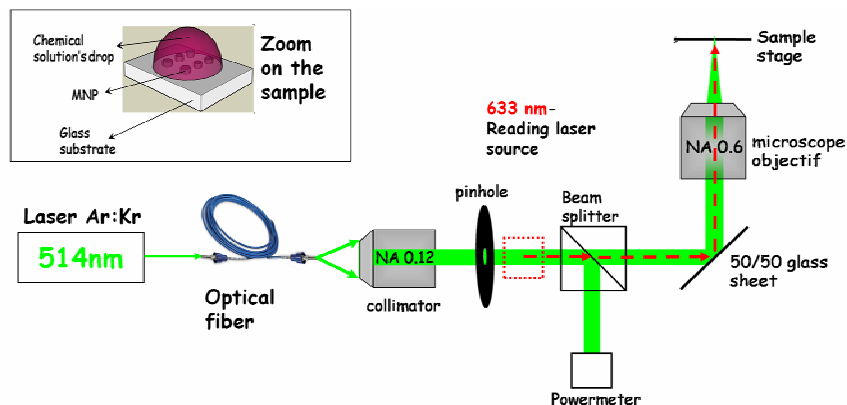

Figure1. Scheme of the newly developed experimental setup.

A He-Ne laser beam, with 633 nm as wavelength, was also coupled in the inverted optical microscope and aligned with the actinic beam. The coupling of this laser offered a reference about the exact position of the Ar:Kr laser spot, even with the presence of the photo-sensitive formulation (Figure 1).

The initial stage of the inverted optical microscope was replaced by a motorized stage of an AFM, Veeco Bioscope II. The optional AFM (with a moveable head) is also coupled to the optical microscope and is monitored by means of a Nanoscope V controller

and an electronic box. The wavelength of the laser beam of the AFM is at 805 nm, meaning that the absorption of the dye will not be influenced by it. Using this new experimental setup, an exposure for a group of metal nanoparticles can be established, then by moving the motorized Veeco stage, a second exposure with different irradiation parameters (power, time, wavelength, *etc*…) may be achieved. Using an appropriate microscope objective, one can also irradiate a single metal nanoparticle. For the results presented in this paper, the optical exposure was performed under normal incidence with a 1-cm wide linearly polarized laser beam from an Ar:Kr laser source, namely 514 nm was used as incident wavelength.

Photopolymerizable organic solutions

The photopolymerizable system used in (Ibn El Ahrach *et al*., 2007) is developed by collaborators at Mulhouse (CNRS UMR 7525) and is consisted of a sensitizer dye (Eosin Y) whose absorption spectrum goes from 450 nm to 550 nm, an amine methyldiethanolamine (MDEA), and a multifunctional acrylate monomer, pentaerythritol triacrylate (PETIA).

Upon the absorption of actinic photons, Eosin is promoted to its singlet state; then, it is converted to its triplet state that undergoes photoreduction by reaction with the amine electron donor (MDEA). The corresponding amine-derived free radicals are now able to initiate polymerization of acrylic monomers. As a result of the propagation and termination steps, the liquid formulation gets converted into a cross-linked polymer, that is a 3D-structure. Reactions involving radicals are highly sensitive to oxygen quenching (Ecoffet *et al*., 1998; Bachelot *et al*., 2001; Espanet *et al*., 1999), leading to an inhibition period. During this period, photons absorbed by the radicals react primarily with dissolved O_2 until a low enough O_2 concentration allows for the polymerization reaction to begin and reach a degree of development enabling subsequent characterization. The amount of energy absorbed by the chemical solution at this stage is defined as the threshold energy (Wurtz *et al*., 2004). A complete characterization of this photopolymerizable formulation has been reported in Deeb *et al*. (2009).

Colloidal nanoparticles CNP and sample preparation

The glass slide was functionalized to create an amine-terminated self-assembled monolayer on which silver nanoparticles of 60-nm diameter, stabilized by citrate groups, were strongly bounded to the glass surface. This enables a well dispersed configuration of commercially synthesized (BBInternational, 2009) colloidal nanoparticles on the substrate surface, as it can be seen on Figure 4(a).

The overall procedure to functionalize the glass slides is detailed in the following and is schematized in Figure 2:

1) Cleaning a glass sheet. The slide is soaked in a freshly prepared piranha solution (2/3 of H_2SO_4 and 1/3 of H_2O_2) at ambient temperature for 2h to remove organic impurities, then it is rinsed thoroughly with water.

2) Aminezation of the slide. The cleaned slide is submerged in a 0.8% amino-silane solution of anhydrous toluene (< 20 ppm of H_2O) for 24h. Then, the glass sheet is removed and rinsed with toluene and acetone to remove unbound materials from the surface. This treatment yields a monolayer of amine grafted to the surface. This

layer is believed to have a thickness of 7A° (Plain *et al*., 2006). Finally, the slide was dried in a stream of dry air. An amine-coated slide was acquired.

3) Attachment of silver nanoparticles to the slide. The amine-coated glass sheet is immersed in the silver colloidal solution for 12h at room temperature to form a self-assembled monolayer of silver nanoparticles, then rinsed with water and dried with air. An atomic force microscopy (AFM) image showing a well distributed configuration CNP grafted to the surface of the amino-silane functionalized glass sheet is shown in Figure 4(a).
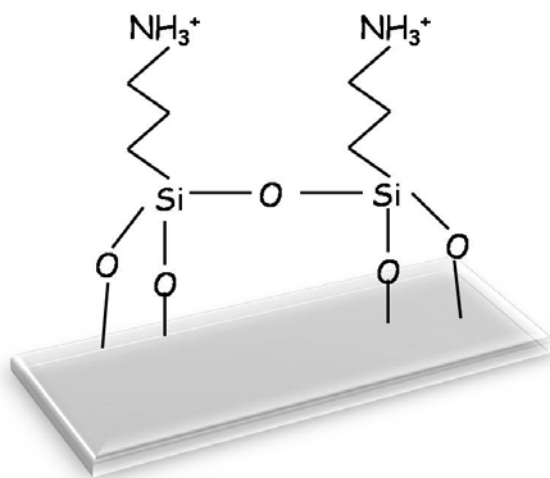

Figure2. Scheme showing the result of the glass slide's functionalization.

This image clearly shows the presence of single CNPs, with 250-nm as typical separation distance, denying all kind of near-field interaction between the nanoparticles. Groups of few particles also exist but no aggregation can be found.

RESULTS AND DISCUSSION

The fabricated CNP samples have been characterized by different techniques: AFM was used to check the shape and size of the deposited particles and extinction and scattering spectroscopy were performed to determine the plasmon resonance position. The diameter of the CNP is deduced from the height of a cross section acquired through the center of a particle, as one can see on the profiles of Figure 5. Since the colloidal particles are spheres, the height acquired from a section sketched along the metal structures represents their diameter. The extinction response of the metallic structures depends on the size, metal nature, shape, and surrounding medium of the CNP. The used silver nanoparticles, of 60-nm diameter, are characterized by a LSP whose wavelength is at 452 nm in water, implying a

LSP of around 465 nm in the monomer solution. An extinction spectrum showing the peak of absorption of CNP is shown in Figure 3.

To selectively address single nanoparticles of well-defined geometry, the decorated glass substrate is placed on an inverted optical microscope that couples to an AFM. Next, the nanoparticles are homogeneously covered by a synthesized free radical photopolymerizable formulation possessing high-resolution visible-light sensitivity and characterized by a threshold dose that must be overcome to induce the polymerization process. A controlled volume of the chemical solution is deposited onto the metal structures using a pipette. A drop of 4-cm diameter, corresponding to a volume of 40 μl, was consistently obtained.
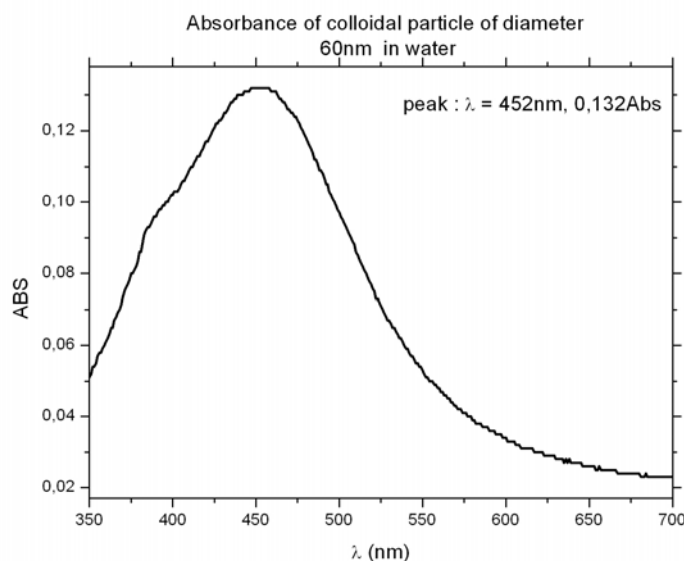
Figure 3. Extinction spectrum of colloidal nanoparticles of 60-nm diameter in water.

The polymerization is activated by laser irradiation with wavelengths overlapping both the photopolymerizable formulation absorption spectrum and the Ag NPs plasmon resonance. The optical exposure is performed under normal incidence with a 1-cm wide linearly polarized laser beam whose wavelength equals 514 nm. The exposure dose is chosen to be smaller than the threshold dose, below which no polymerization can occur. This threshold value is systematically quantified by far-field pre-studies (Ibn El Ahrach *et al.*, 2007; Deeb *et al.*, 2009). Therefore, photopolymerization is not expected to occur in the absence of Ag NPs: because of the field enhancement at the plasmon resonance, the effective dose near the metallic nanoparticles can be greater than the threshold to initiate the chain reaction leading to polymerization.

After irradiation, any monomer that is not reticulated is removed by a rinsing procedure with ethanol and isopropanol and characterized by AFM using intermittent-contact mode. It should be stressed that AFM characterization before and after the exposure is

performed for the same pre-selected individual Ag NP. The coupled AFM-inverted optical microscope allows one to address single labeled particles and to retrieve them after the rinsing procedure. After rinsing and re-characterization, the metal particles exhibit an elongation along the direction of the incident electric field. This elongation results from the photopolymerization initiated by the enhanced local field and directed parallel to the incident polarization.

The aim of changing the laser energy between two successive exposures is to have a parametric study of the created polymer parts that are related to the CNP's near field intensity distribution.

Figure 4(a) shows an AFM image of CNP before exposure, while the AFM image 4(b) shows the CNP after being exposed with a dose equal to 75% of the threshold dose. A single isolated particle was chosen (circle) to demonstrate one's ability to map the field down to sub-10-nm resolution. Due to tip convolution, its apparent diameter is 110 nm while its actual diameter is 60 nm as deduced from the height of a cross section acquired through the center of the CNP (Figure 5). The encircled particle exhibits an elongation along the y-direction that results from the photopolymerization prompt by the enhanced local near-field. It should be highlighted that both panels of Figure 4 were obtained with the same tip under the same scanning conditions. This elongation, clearly seen in the cross section done along the Y-direction which is the direction of the incident beam, is due to two symmetric polymer lobes built up close to the particles resulting in metal-polymer hybrid particles. The two lobes originate from the dipolar excitation of CNP's surface plasmon resonance. The field distribution associated with the resonance is enhanced in a two-lobe region oriented with the incident polarization. The localized nanoscale photopolymerization is the result of the inhomogeneous field distribution.
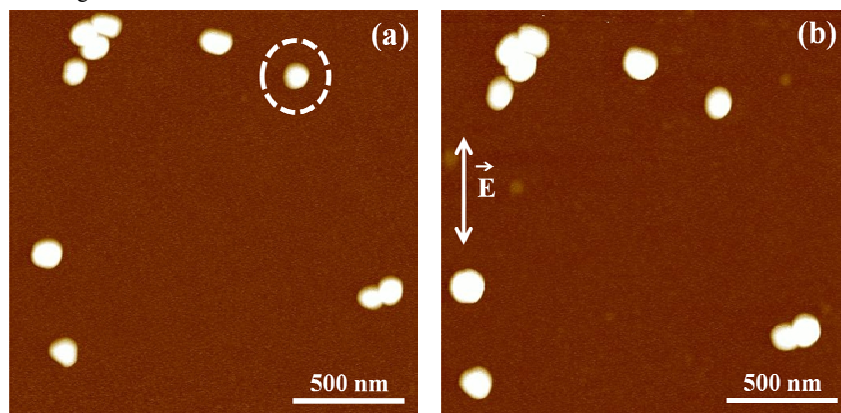

Figure 4. AFM image 2μmx2μm of CNP before exposure (a) and after being exposed with photopolymerizable solution (b).

The elongation of the CNP in the direction of the incident field is illustrated in Figure 5. Panels (a) and (b) of this figure show the profile of the circled particle in the AFM image 4(a) before and after the procedure, respectively. The sections were done along the X-

and the Y-direction and were equal to 10 nm and 40 nm, respectively. The cross sections were performed along both directions to reveal the highest elongation of the particle along the Y-direction which was the direction of the incident polarization. However, the elongation of the CNP along the X-direction is due to a residual monomer solution that remain stuck on the particle.
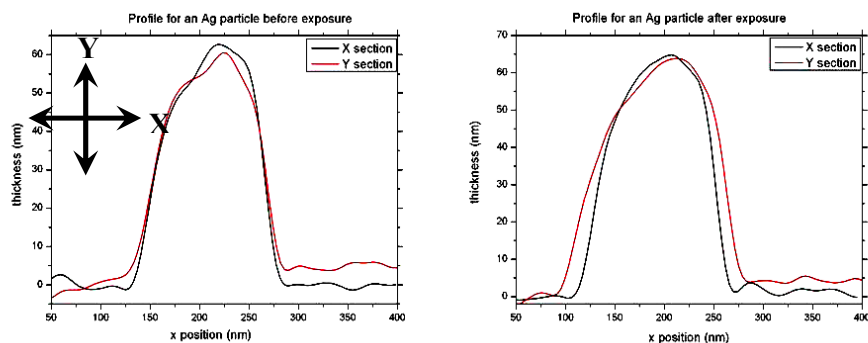

Figure 5. Profile of the circled particle of image 4(a) before and after being exposed. The sections were done along the X- and the Y-direction.

In order to highlight the localized photopolymerization, the AFM image of the encircled particle before the procedure is substracted from the AFM image of the same particle after the procedure. The differential image, shown in Figure 6, clearly reveals two polymer wings oriented along the incident polarization direction. The two lobes of polymer, originating from the dipolar excitation of CNS's surface plasmon resonance, are resulting from the inhomogeneous distribution of the CNP's near field. Such differential image accurately depicts the spatial distribution of the polymerization resulting from the reticulation process, while circumventing the apparent increase of the polymer depth due to convolution with the AFM tip. This is why it is possible to see the exact spatial extension of polymer on this Figure and that is approximately equal to 40 nm, in opposition to the case where the tip convolution was present (Figure 5).
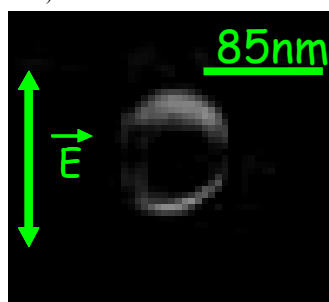

Figure 6. Result of the subtraction between the "after" and the "before" AFM images of the circled particle in Figure 4(a). This figure clearly shows the lobes of polymer in the direction of the incident polarization.

In order to quantify the local field enhancement of this type of metallic nanoparticles, the laser incident dose was varied and the influence of this parameter on the elongation of the CNP in the direction of the incident polarization was studied. The incident dose was chosen to be equal one quarter, one half and three quarter of the threshold dose. As one can expect, Figure 7 shows that the elongation of the CNP, in the direction of the incident electric field polarization, increases whenever the incident dose increases. It is worth noticing that an elongation of 15 nm is recorded for an incident dose that is equal to the quarter of the threshold one. This implies that the CNP are able to enhance the incident electric field by, at least, 4 times since a measurable elongation was seen at this dose. Moreover, this suggests to reduce the incident dose to 20%, 15%, 10% and even 5% of the threshold dose and to check for every single dose the corresponding CNP elongation. Following this procedure, one can guarantee a precise determination of the enhancement factor of this type of metal structure.
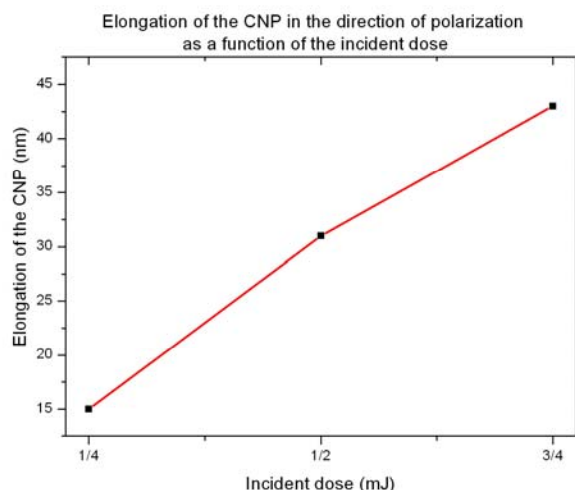

Figure 7. Elongation of the CNP in the direction of the incident polarization as a function of 25% = 1/4, 50% = 1/2 and 75% = 3/4 of the threshold dose.

CONCLUSIONS AND PERSPECTIVES

In conclusion, what was demonstrated was controlled nanoscale photopolymerization in the near-field of resonant metal nanoparticles. In this paper, what is shown is the ability to map the evanescent optical near-field supported by resonant LSP of individual silver nanoparticles, with sub-10-nm resolution. As was elucidated, this approach relies on exploiting the enhancement of the electric field around a resonantly excited silver nanoparticle to trigger local photopolymerization, resulting in a polymer mold, which directly profiles the dipolar near-field distribution around the particle. The resolution with which one is able to profile the near-field is unprecedented (sub-10-nm). To the best of one's knowledge, this is the first time, a sub-10 nm resolution photo-polymerization is being demonstrated in the visible, allowing, in turn, a sub-10 nm optical resolution characterization of plasmonic structures.

Additionally, this approach constitutes a novel technique to determine precisely the enhancement factor of the enhanced near-field of metal nanostructures. Such experiments to quantify fields enhancement factors values are under way. Finally, the used technique opens new routes for nanophotochemistry and it also offers a hybrid metal/polymer structure with new optical properties.

ACKNOWLEDGEMENTS

REFERENCES

Atwater, H.A. and Polman, A. 2010. Plasmonics for improved photovoltaic devices. *Nature Materials,* (9): 205-213.

Bachelot, R., Eoffet, C., Deloeil, D., Royer, P. And Lougnot, D.J. 2001. Integration of micrometer-sized polymer elements at the end of optical fibers by fee-radical photopolymerization. *Applied Optics,* (40): 5860-5871.

Bachelot, R., H'Dhili, F., Barchiesi, D., Lerondel, G., Fikri, R., Royer, P., Landraud, N., Peretti, J., Chaput, F., Lampel, G., Boilot, J.P. and Lahlil, K. 2003. Apertureless near-field optical microscopy: A study of the local tip field enhancement using photosensitive azobenzene-containing films. *Journal of Applied Physics,* (94): 2060.

Barnes, W.L., Dereux, A. and Ebbesen, T. 2003. Surface plasmon subwavelength optics. *Nature,* (424): 824-830.

Bouhelier, A., Bachelot, R., Lerondel, G., Kostcheev, S., Royer, P. and Wiederrecht, G.P. 2005. Surface plasmon characteristics of tunable photoluminescence in single gold nanorods. *Physics Review Letters,* (95): 267405.

Deeb, C., Baudrion, A.-L., Jradi, S., Plain, J., Bouhelier, A., Sopppera, O., Balan, L., Ridaoui, H., Royer, P. and Bachelot, R. 2009. Nanoscale poto polymerization induced by the enhanced optical near field of metallic nanoparticles. *Proceeding of SPIE 7395,* 739505, San Diego, USA.

Ecoffet, C., Espanet, A. And Lougnot, D.J. 1998. Photopolymerization by evanescent waves: a new method to obtain nanoparts. *Advanced Materials,* (10): 411-414.

Espanet, A., Dos Santos, G., Ecoffet, C., and Lougnot, D.J. 1999. Photopolymerization by evanescent waves: characterization of photopolymerizable formulation for photolithography with nanometric resolution. *Applied Surface Science,* (138): 87-92.

Haes, A.W., Hall, W.P., Chang, L., Klein, W.L. and Van Duyne, R.P. 2004. A localized surface plasmon resonance biosensor: first steps toward an assay for Alzheimer's disease. *Nano Letters,* (4): 1029-1034.

Ibn El Ahrach, H., Bachelot, R., Vial, A., Lerondel, G., Plain, J., Royer, P. And Soppera, O. 2007. Spectral degeneracy breaking of the plasmon resonance of single metal nanoparticles. *Physics Review Letters,* (98): 107402.

Noginov, M.A., Zhu, G., Belgrave, A.M.., Bakker, R., Shalaev, V.M., Narimanov, E. 2009. Demonstration of a spaser-based nanolaser. *Nature,* (460): 1110-1112.

Plain, J., Pallandre, A., Nysten, B. and Jonas, A. 2006. Nanotemplated crystallization of organic molecules. *Small,* (2): 892-897.

Schuller, J.A., Barnard, E.S., Cai, W., Jun, Y.C., White, J.S. and Brongersma, M.L. 2010. Plasmonics for extreme light concentration and manipulation. *Nature Materials,* (9): 193-204.

Wurtz, G., Burget, D. and Carré, C. 2004. Photopolymerization induced materialization of the dipolar response from isolated metallic nanoparticles. *SPIE, (39):* 278-286.

Zayat, A.V. and Smolyaninov, I.I. 2003. Near-field photonics: surface plasmon polaritons and localized surface plasmons. *Journal of Optics A: Pure and Applied Optics,* (5): 16-50.